Applied Surface Science xxx (2014) xxx–xxx

Contents lists available at ScienceDirect

Applied Surface Science

journal homepage: www.elsevier.com/locate/apsusc

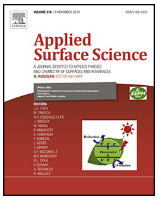

Near-infrared to visible and near-infrared upconversion of monoclinic Gd_2O_3:Yb^{3+}/Tm^{3+} nanoparticles prepared by laser ablation in liquid for fluorescence imaging

Jun Liu [a], Xiumei Tian [b], Hongpeng Chen [a], Yuanzhi Shao [a], Guowei Yang [a], Dihu Chen [a,*]

[a] *State Key Laboratory of Optoelectronic Materials and Technologies, Sun Yat-sen University, Guangzhou 510275, PR China*
[b] *Department of Biomedical Engineering, Guangzhou Medical University, Guangzhou 510182, PR China*

ARTICLE INFO

Article history:
Received 23 September 2014
Received in revised form
17 November 2014
Accepted 19 November 2014
Available online xxx

Keywords:
Upconversion nanoparticles (UCNPs)
Fluorescence imaging
Deep tissue penetration
Laser ablation in liquid (LAL)

ABSTRACT

Upconversion nanoparticles (UCNPs) possess great potential for application in fluorescence imaging. Here, the high crystalline Gd_2O_3:Yb^{3+}/Tm^{3+} UCNPs with the average diameter of 7.18 nm were fabricated by laser ablation in liquid (LAL). Under excitation at 980 nm, visible blue fluorescence of the LAL-derived Gd_2O_3:Yb^{3+}/Tm^{3+} UCNPs is obtained and can be used for live cells imaging. Meanwhile, more efficient near-infrared (NIR) emission (~800 nm) than the visible fluorescence is observed. The excitation and emission of Gd_2O_3:Yb^{3+}/Tm^{3+} UCNPs are both within the "optical transmission window" of biological tissue, capable of great potential for deep tissues imaging.

1. Introduction

Lanthanide-doped fluorescence nanoparticles have attracted considerable interest in biomedical application research due to their excellent chemical and optical properties compared with traditional fluorescence probes (organic dyes and semiconductor quantum dots), including low cytotoxicity, large stocks shifts, sharp emission bandwidths, and high resistance to photobleaching and photochemical degradation [1,2]. However, the lanthanide-doped nanoparticles with down-conversion fluorescence, which are excited by ultraviolet (UV) or visible light, is limited by their strong background autofluorescence, tissue photodamage, and low tissue penetration [3]. Nanoparticles with upconversion fluorescence, which are excited by the near-infrared (NIR) light, have attracted much attention biomedical application [4–6]. Compared with UV–vis light, the NIR light excitation can penetrate biological tissue more efficiently because these tissues scatter and absorb less light at longer wavelengths, and produce low autofluorescence and less photodamage [7–9].

For upconversion materials, a sensitizer with a sufficient absorption cross-section in NIR region is usually co-doped with the activator in host materials to enhance the upconversion efficiency [10]. For sensitizer/activator, the Yb^{3+}/Er^{3+}, Yb^{3+}/Ho^{3+}, and Yb^{3+}/Tm^{3+} ion pairs are identified to be the most efficient combinations to yield visible emission, when excited at ~980 nm [11]. Note that the Yb^{3+}/Tm^{3+} co-doped upconversion nanoparticles (UCNPs) possess efficient NIR (~800 nm) emission under excitation at ~980 nm [12–15], where the excitation and emission are both within the "optical transmission window" of biological tissue. It means that they can act as the excellent fluorescence nanoprobes for deep tissues imaging [3,16]. Among the host materials, fluorides and oxides are most frequently used at present. Fluorides generally exhibit higher upconversion efficiency because of their low nonradiative losses than that of oxides [17]. Nonetheless, the toxicity of fluorine is needed to be concerned. Thus, the low toxicity and desirable chemical stability of oxides makes them more suitable for biomedical applications. Among these oxides, ytterbium oxide (Y_2O_3) and gadolinium oxide (Gd_2O_3) are most popular host materials due to their low phonon energy [18,19].

Conventional techniques for preparing the lanthanide-doped nanoparticles are chemical routes (precipitation, sol–gel, hydrothermal methods, etc.) [20–24]. However, the chemical strategies are not only complicated, but also cause additional toxicity for human body due to the presence of residual chemicals [25,26]. The laser ablation in liquid (LAL) has been established as a reliable and efficient approach for preparing high-purity nanoparticles, such as semiconductors [27,28], noble metals [29–31], and

---

* Corresponding author. Tel.: +86 20 13600452080; fax: +86 20 84113398.
E-mail address: stscdh@mail.sysu.edu.cn (D. Chen).

http://dx.doi.org/10.1016/j.apsusc.2014.11.105

Please cite this article in press as: J. Liu, et al., Near-infrared to visible and near-infrared upconversion of monoclinic Gd_2O_3:Yb^{3+}/Tm^{3+} nanoparticles prepared by laser ablation in liquid for fluorescence imaging, Appl. Surf. Sci. (2014), http://dx.doi.org/10.1016/j.apsusc.2014.11.105

metal oxides [32], without the use of any chemical precursors or other organic reagents. Thus, the obtained colloids are 100% pure, which are suitable to produce lanthanide-doped nanoparticles for biomedical application. Wada's group and Singh's group have reported the synthesis of the Y_2O_3:Yb^{3+}/Er^{3+} and Gd_2O_3:Yb^{3+}/Er^{3+} UCNPs by LAL technique, which show that the LAL-derived UCNPs possess high crystalline and efficient upconversion emission [33–36]. Our previous works have focused on the fabrication of Gd_2O_3 nanoparticles as magnetic resonance imaging (MRI) contrast agents by LAL technique [37,38], and evaluated their biological toxicity [39]. Recently, we reported the fabrication of lanthanide-doped Gd_2O_3 nanoparticles with down-conversion fluorescence as dual-modal contrast agents [40,41]. We also noticed that the Gd_2O_3 in our studies is usually monoclinic phase, which is hard to obtain by traditional chemical routes and possess superior UC efficiency than that of the cubic phase due to its lower symmetry of crystal field [42,43].

In this paper, the Gd_2O_3:Yb^{3+}/Tm^{3+} UCNPs were fabricated by the LAL technique in deionized water and applied as upconversion fluorescence probes. The structure, morphology, component, and optical performance of the Gd_2O_3:Yb^{3+}/Tm^{3+} UCNPs are studied. Stronger NIR emission than the visible light is observed under excitation at ~980 nm. This suggested that the LAL-derived Gd_2O_3:Yb^{3+}/Tm^{3+} UCNPs have great potential for application in deep tissues fluorescence imaging.

2. Materials and methods

2.1. Preparation and characterization of Gd_2O_3:Yb^{3+}/Tm^{3+} UCNPs

Gd_2O_3, Yb_2O_3, and Tm_2O_3 powders of analytical grade with a stoichiometric ratio of 83:15:2 were used for the preparation of Gd_2O_3:Yb^{3+}/Tm^{3+} target *via* standard solid state reaction techniques. The details have been reported in our previous work [40]. Then the Gd_2O_3:Yb^{3+}/Tm^{3+} UCNPs were synthesized by laser ablation of the target in deionized water. The laser system used in this study is a commercial high energy microsecond Nd:YAG laser with a wavelength of 1064 nm, a pulse duration of 6 μs, a repetition of 100 Hz, and a power of 70 mJ/pulse. The ablation process lasted for 15 min. The ablated colloids were aged for 24 h; then, the upper aqueous suspension was collected.

One drop of a fresh aqueous suspension of the products was placed on a carbon-coated copper grid and prepared for the transmission electron microscope (TEM, JEOL JEM-2010HR, Japan) observation. Several drops of aqueous suspension were placed on two silicon wafers, and then dried at 50 °C; this process repeated many times until a thin white layer was formed. Samples were characterized by X-ray diffractometer (XRD, D-MAX2200 VPC, Japan) and X-ray photoelectron spectrometer (XPS, ESCALab250, USA). The upconversion fluorescence spectrum of the products was measured by Edinburgh spectrofluorophotometer (FLS920, UK) at room temperature, equipped with a 980 nm NIR laser.

2.2. Cell culture and live cells fluorescence imaging

The murine macrophage cell line (Raw264.7 cells) was grown at 37 °C under 5% CO_2 in Dulbecco's modified Eagle's medium (DMEM) containing 10% fetal bovine serum (FBS), penicillin (100 units/ml), and streptomycin (100 mg/ml). The cells were incubated with the Gd_2O_3:Yb^{3+}/Tm^{3+} UCNPs for 2 h. After co-incubation, the cells were washed with PBS to remove the remaining particles and dead cells, and then observed under a laser scanning confocal microscope (Zeiss LSM 710, Germany), operating at 980 nm NIR excitation wavelength.

2.3. Cytotoxicity assay

The CNE-2 and NP69 cells were incubated with different Gd concentrations (10, 5, and 2.5 μM) of the Gd_2O_3:Yb^{3+}/Tm^{3+} UCNPs in 96-well plates and treated with culture media as negative control (A group that has not been administered any drug or nanoparticles and should show a negative or null toxic effect) and lipopolysaccharide (LPS) as positive control (A group that the toxicity is expected), all groups were cultured for 48 h. After co-incubation, 20 μL of [3-4,5-dimethyl thiazol-2-yl]-2,5-diphenyltetrazolium bromide succinate (MTT) was added for another 4 h of incubation. Then, all the culture medium was removed and 100 μL of dimethyl sulfoxide (DMSO) was added to dissolve the formazan crystals for 10 min, and the absorbance was measured by a microplate reader (Bio-Rad, USA) at 490 nm.

3. Results and discussion

The typical TEM image in Fig. 1a shows that the as-prepared nanoparticles possess a nearly spherical shape. The HRTEM image (Fig. 1b) and the corresponding SAED pattern (insert in Fig. 1b) is the evidence of its polycrystalline structure. As shown in Fig. 1c, the interplanar spacing of nanocrystals is measured to be about 0.310 nm, which corresponds to the *d* value of the (1 1 1) crystallographic plane of monoclinic Gd_2O_3 (d_{111} = 0.316 nm, PDF#42-1465). Fig. 1d displays the corresponding size distribution histogram, indicated the average diameter of the as-prepared nanoparticles is approximately 7.18 nm.

The crystal structure of the nanoparticles is further identified by the XRD measurement, as shown in Fig. 2. It could be observed that the peaks of the nanoparticles match well with the monoclinic Gd_2O_3 (PDF#42-1465), and no obvious impurity phases are detected. Note that the strong and narrow peaks of XRD indicate the good crystallinity of the nanoparticles. To further confirm the components of the nanoparticles, XPS was conducted and the high-resolution spectra of the samples are showed in Fig. 3. Peaks at 1221.7, 1187.8, 146.20 and 141.80 eV denoted $Gd3d_{3/2}$, $Gd3d_{5/2}$, $Gd4d_{3/2}$, and $Gd4d_{5/2}$, respectively, and peaks at 184.80 and 170.70 eV denote Yb4d, and Tm4d, respectively. The corresponding XRD and XPS results demonstrate that Yb^{3+}/Tm^{3+} ions are successfully co-doped in Gd_2O_3 host matrix.

Fig. 4a shows the upconversion fluorescence emission spectrum of Gd_2O_3:Yb^{3+}/Tm^{3+} UCNPs at the range of 405–900 nm under excitation at 980 nm. The inset in Fig. 4a is the corresponding magnified part of the visible light emissions. Clearly, the Gd_2O_3:Yb^{3+}/Tm^{3+} UCNPs show a blue emission at around 481 nm, two red emissions at around 658 and 700 nm, and it is striking that the NIR emission peaked at 801 nm is much more intense than all the other upconversion fluorescence bands. Fig. 4b shows the digital photograph of the Gd_2O_3:Yb^{3+}/Tm^{3+} UCNPs colloid, take without and with 980 nm excitation (no optical filters were used). Naked-eye compatible blue fluorescence is observed. Fig. 5a shows the schematic illustration of upconversion emission process in Gd_2O_3:Yb^{3+}/Tm^{3+} UCNPs and the random energy transfer (ET) among the Yb^{3+} and Tm^{3+} ions. Under NIR excitation at 980 nm, the Yb^{3+} continuously absorbed 980 nm photons due to its large absorption cross section, and then transfers the energy to the Tm^{3+} ions, resulting in different photon emissions. Fig. 5b shows the schematic energy level diagrams of Yb^{3+} and Tm^{3+}, as well as the possible upconversion mechanism. Firstly, the ground state electronics of Tm^{3+} ions obtain energy *via* ET1 from neighboring Yb^{3+} and populate the state of $^3H_5$, then nonradiative relaxed to the state of $^3F_4$. The electronics in the $^3F_4$ state can be further excited to the $^3F_2$ state *via* ET2, and populate the state of $^3F_3$ or $^3H_4$ by nonradiative relaxation. Subsequently, the electronics in $^3H_4$ level can populate the $^1G_4$ level *via* ET3. As these

Please cite this article in press as: J. Liu, et al., Near-infrared to visible and near-infrared upconversion of monoclinic Gd_2O_3:Yb^{3+}/Tm^{3+} nanoparticles prepared by laser ablation in liquid for fluorescence imaging, Appl. Surf. Sci. (2014), http://dx.doi.org/10.1016/j.apsusc.2014.11.105